# Lifetimes of Excited States of Nuclei with Odd Mass*

R. E. HOLLAND AND F. J. LYNCH
*Argonne National Laboratory, Lemont, Illinois*
(Received October 24, 1960)

The lifetimes of Coulomb-excited states in $Ti^{47}$, $Mn^{55}$, $Fe^{57}$, $Zn^{67}$, $Ge^{73}$, $Se^{77}$, and $Mo^{95}$ have been measured by a pulsed-beam technique. The observed mean lifetimes were between 0.1 and 12.7 m$\mu$sec. By combining these data with the measured Coulomb-excitation cross sections, we obtained the partial mean life for magnetic-dipole radiation and the ratio $(E2/M1)$ for these transitions. The partial $M1$ lifetimes are 20 to 200 times as long as the single-particle estimates.

## I. INTRODUCTION

IN this paper we describe the measurement[1] of the lifetime of levels that can be reached by Coulomb excitation in odd-mass nuclei. From these measurements we can obtain the ratio of electric-quadrupole to magnetic-dipole radiation in the decay of the state as well as the partial transition rates for electric-quadrupole and magnetic-dipole radiation.

For these excited states in odd-mass nuclei, a spin difference of two between excited state and ground state allows only quadrupole or higher order radiation. For these transitions only the electric-quadrupole transition is important and the observed lifetime (allowing for internal conversion) should be equal to the $E2$ lifetime deduced from the Coulomb-excitation cross section. In many cases, however, in odd-mass nuclei the spin of the excited state differs from that of the ground state by one or zero. Here, both electric-quadrupole ($E2$) and magnetic-dipole ($M1$) radiation are allowed. The observed decay constant of these states may be written as

$$\lambda(\text{obs})=\lambda(E2)(1+\alpha_2)+\lambda(M1)(1+\beta_1), \qquad (1)$$

where $\lambda(E2)$ and $\lambda(M1)$ are the partial decay rates for electric-quadrupole and magnetic-dipole radiation and $\alpha_2$ and $\beta_1$ are the corresponding internal-conversion coefficients. Usually only $\lambda(E2)(1+\alpha_T)$, where $\alpha_T$ is the total internal-conversion coefficient, is known from the cross section for Coulomb excitation since the internal-conversion coefficient has not been measured. By using the relation

$$\alpha_T=\frac{\alpha_2\lambda(E2)+\beta_1\lambda(M1)}{\lambda(E2)+\lambda(M1)},$$

and the measured quantities $\lambda(\text{obs})$ and $(1+\alpha_T)\lambda(E2)$ together with theoretical values[2] for $\alpha_2$ and $\beta_1$, we have three independent equations with three unknowns. The solution of these equations gives $\lambda(E2)$, $\lambda(M1)$, and $\alpha_T$ as well as the ratio $\lambda(E2)/\lambda(M1)\equiv(E2/M1)$. The latter quantity may be compared to the values obtained by measuring the internal-conversion coefficients or by measuring the angular correlation. In one case only $E2$ radiation was allowed and here we could compare our results directly with that obtained from the measured cross section for Coulomb excitation.

The procedure used in these experiments was the following. In each case a gamma ray from a state with very short lifetime was observed alternately with the gamma ray from the state whose lifetime was to be measured. The data from the short-lived state gave the time resolution of the system. These two sets of data were then analyzed to obtain the lifetime of the unknown state. Sources of systematic error were investigated in some detail. A description of the method of measurement, an analysis of the data, a discussion of the sources of systematic error, and the results follow.

## II. EQUIPMENT

These measurements were made with an externally pulsed beam of singly-ionized $He^4$ ions from the 4-Mev electrostatic accelerator at Argonne National Laboratory.[3] Pulses were produced by passing the beam between two plates which were part of a resonant circuit driven in most cases at 7.5 Mc/sec. The beam pulses produced had a width of 0.7 m$\mu$sec as determined from the reduction in average target current when the deflecting voltage was applied. The average current at the target after pulsing could be as large as 0.3 $\mu$a, but it was usually less than this in order to reduce electronic effects which occurred when the counting rate was high.

The detector consisted of a NaI(Tl) scintillator, usually $\frac{1}{4}$ in. thick and 1 in. in diameter, connected by a Lucite light pipe $\frac{3}{4}$ in. long to an RCA-7251 photomultiplier tube. Some data were also taken with scintillators $\frac{1}{8}$ in. thick and $\frac{1}{2}$ in. thick, both with and without a light pipe. We monitored the anode current of the photomultiplier and kept the anode current below 0.2 $\mu$a to limit fatigue effects in the photomultiplier tube. The output of the phototube was amplified by two Hewlett Packard 460A distributed amplifiers

* This work was performed under the auspices of the U. S. Atomic Energy Commission.

[1] Preliminary reports of this work have been given by F. J. Lynch and R. E. Holland, Bull. Am. Phys. Soc. 3, 380 (1958); R. E. Holland and F. J. Lynch, Bull. Am. Phys. Soc. 4, 232 (1959).

[2] R. E. Rose, *Internal Conversion Coefficients* (North-Holland Publishing Company, Amsterdam, 1958).

[3] Additional experimental details are given in previous papers: R. E. Holland and F. J. Lynch, Phys. Rev. **113**, 903 (1959); F. J. Lynch and R. E. Holland, Phys. Rev. **114**, 825 (1959); R. E. Holland, F. J. Lynch, and S. S. Hanna, Phys. Rev. **112**, 903 (1958).

before being presented to the trigger circuit of a time-to-pulse-height converter. The triggering level of this circuit corresponded to 3 photoelectrons in most cases. A parallel slow amplifier and single-channel analyzer were used to gate the 256-channel analyzer which stored the pulses from the time-to-pulse-height converter. The 256-channel analyzer was used as two 128-channel analyzers and pulses from the time-to-pulse-height converter were stored in one or the other depending on which of two targets was under observation. Targets and storage were changed automatically upon a signal from a beam-current integrator set to accept a fixed amount of beam charge. This procedure gave a first-order cancellation of drift in the electronic equipment. Both the target assembly and the detector were enclosed in a lead box 18 in.×15 in.×24 in. and with walls $\frac{1}{2}$ in. thick. The interior of the box was lined with iron plate $\frac{1}{4}$ in. thick which acted as a filter for the 75-kev $K$ x rays produced in the lead by the absorption of higher energy gamma rays. The shield was effective in reducing the background of low-energy x rays produced by the accelerator.

In this work it was essential to obtain a "prompt" time spectrum, corresponding to a short-lived state, by bombarding a target under conditions identical to those used to obtain the time spectrum of the state under investigation. This prompt time spectrum then gave the time resolution of the system. If possible, the energy of the prompt gamma ray should be close to the energy of the state whose lifetime is to be measured. In the region below 80 kev, one may use x rays as comparison sources. For higher energies, no targets are available to supply gamma rays that have arbitrary energy and are known to come from a state with very short lifetime (less than $10^{-11}$ sec). In the latter case we have used the Compton pulses from the 480-kev gamma ray from the first excited state of $Li^7$ (mean life[4] $7.7\times10^{-14}$ sec), which is easily excited by $\alpha$-particle bombardment of a thin Li target. Except for the lithium targets, the targets used in this work were thick and of normal isotopic composition. Two targets were mounted in an assembly which allows either to be placed in the beam.

Calibration of the time-to-pulse-height converter was made in the following manner. The full time spectrum from the converter was recorded with a prompt target. The time between gamma-ray peaks of this double display of the time spectrum is very close to half the period of the rf deflecting voltage. By delaying the signal from the detector, the peaks could be reversed and the other half of the rf cycle measured. The calibration was taken from the average of these two measurements. Deviation of the measurements from the mean was less than 2%. Over a period of two weeks, the calibration was checked daily and remained within 1% of the mean.

A series of measurements consisted of (1) observing the pulse-height spectrum of the NaI scintillation counter and setting the window of the single-channel analyzer to correspond to a particular photopeak; and (2) recording a pair of time spectra (one from the "unknown" target and one from the prompt target) in the two halves of the 256-channel analyzer. The targets were alternated after accumulation of a definite amount of charge from the beam (which required approximately 1 min).

Backgrounds were determined from the counting rate in channels far from the peak in the time spectrum. In a typical case the background was one count per channel compared to 500 counts per channel at the peak of the time spectrum. After subtraction of background, the data were analyzed according to the procedures described in Sec. III.

## III. ANALYSIS OF DATA

Analysis of the data from this experiment was based on the equation[5] which describes the folding of the prompt curve (giving the over-all time resolution) with the decay function $f(t)$, namely,

$$d_f(t)=\int_0^\infty f(t')P(t-t')dt'. \tag{2}$$

Here $d_f(t)$ is the curve to be expected for a state decaying according to $f(t)$, and $P(t)$ is the prompt curve. We have used the methods of analysis described below, one of which is new.

One well-known method obtains the mean life from the centroids of the prompt and unknown time spectra. If one knows that the delayed time spectrum is due to a simple decay of the form $e^{-\lambda t}$, it has been shown[5] that

$$\tau=\frac{1}{\lambda}=\frac{M_1(D)}{M_0(D)}-\frac{M_1(P)}{M_0(P)},$$

where $M_0(P)$, and $M_1(P)$ are the zeroth and first moments of the measured prompt time spectra and $M_0(D)$ and $M_1(D)$ are the corresponding moments for the measured delayed time spectra. Similar expressions can be developed for higher moments and we have relations involving moments as high as the fifth for computations of this sort. The presence of unsuspected components of other lifetimes makes itself felt in these computations by a deviation in the computed value of $\tau$ as higher moments are used, since they weight the tail of the time spectrum more heavily.

Monahan[6] has developed a second method based on the method of least squares. By use of Eq. (2), the delayed spectra for an arbitrary mean life $\tau$ may be calculated from the prompt spectra; and by using an iterative procedure one may then search for that value

[4] F. Ajzenberg-Selove and T. Lauritsen, Nuclear Phys. **11**, 1 (1959).

[5] Z. Bay, Phys. Rev. **77**, 419 (1950).

[6] J. E. Monahan (unpublished).

of $\tau$ which minimizes

$$Q=\sum_j \frac{|D(j)-d(j)|^2}{[\sigma(j)]^2},$$

where $D(j)$ is the measured count in channel $j$ of the delayed spectrum, $d(j)$ is the corresponding quantity for the spectrum calculated from the observed prompt spectrum $P(j)$ according to Eq. (2), and $\sigma(j)$ is a statistical weight based on $D(j)$ and $P(j)$. The calculated values of $d(j)$ which minimize $Q$ are plotted in the figures in Sec. IV of this paper. From this analysis one obtains values of $\chi^2$ and of an error to be associated with the $\tau$ which best fits the data. This computed error in $\tau$ is smaller than that derived from the centroid computations; it does not reflect strongly errors due to the presence of other gamma rays or other systematic effects. Such systematic errors, however, do make themselves felt as nonrandom variations between the computed and observed spectra $d(j)$ and $D(j)$. In some cases (see discussion of $Zn^{67}$ in Sec. IV), the behavior of the variations between $D(j)$ and $d(j)$ was investigated in some detail. The frequency distribution of the quantity $[D(j)-d(j)]/E(j)$, where $E(j)$ is the expected error in $[D(j)-d(j)]$, was a Gaussian curve. In general the values of $\chi^2$ were larger than the expected mean values but less than the expected value for a 1% chance of occurrence, even for cases where some systematic errors were known to be present.

In applying Eq. (2) or relations derived from it, one is not always allowed to simply replace the integral by a summation over channels. This procedure was satisfactory for the moment computations but in applying the least-squares fitting procedure, Eq. (2) was replaced by

$$d(j)=\frac{1+\lambda-e^{\lambda}}{\lambda}P(j)+\frac{e^{\lambda}+e^{-\lambda}-2}{\lambda}\sum_{k=1}^{j}P(k)e^{\lambda(k-j)},$$

when $f(t)=\lambda e^{-\lambda t}$.

A simple least-squares fit of an exponential function to the tail of the delayed time spectrum was used in those cases in which the ratio of lifetime to resolution time was large enough. Although the statistical accuracy was usually low for our data, this method was not subject to some of the difficulties involved in those described in the following section.

## IV. RESULTS

Table I summarizes the data for the nuclei which we have studied. The columns give the isotope, the excitation energy of the state, the spin of the ground state, the reduced (upward) transition rate $B(E2)$ from the cross section for Coulomb excitation from other experiments, the partial mean life for a downward $E2$ transition as deduced[7] from $B(E2)$, the experimental mean life, the $E2$ conversion coefficient, the $M1$ conversion coefficient, the partial $M1$ mean life, the ratio $\tau(M1)/\tau(E2)$, and a calculated value for the mean life. The meaning of this calculation is described in detail in the discussion of individual cases below.

The spins of the ground states and excited states must be known in order to obtain $\tau(E2)$ from $B(E2)$.

TABLE I. Summary of results of lifetime measurements. Listed are the isotope, energy of excitation of the level, spin and parity of ground state, spin and parity of excited state, reduced transition probability (uncorrected for internal conversion) taken from the work of others, the observed mean life, partial mean lives for $E2$ and $M1$ decay, the conversion coefficients used in the calculations, the ratio $\lambda(E2)/\lambda(M1)$, and the mean life (for $Fe^{57}$) calculated from other data.

| Isotope | Energy of excitation kev | $I_0$ | $I_{ex}$ | $\epsilon B(E2)$ $(10^{-48})$ $cm^4$ | $\tau$(obs) m$\mu$sec | $\tau(E2)$ m$\mu$sec | $\tau(M1)$ m$\mu$sec | $\alpha_2$ | $\beta_1$ | $(E2/M1)$ | $\tau$(calc) m$\mu$sec |
|---|---|---|---|---|---|---|---|---|---|---|---|
| $Ti^{47}$ | 160 | $\frac{5^-}{2}$ | $\left(\frac{7^-}{2}\right)$ | 0.040[a] | 0.32±0.10 | 25.7 | 0.326 | 0.054 | 0.0053 | 0.013 | ··· |
| $Mn^{55}$ | 128 | $\frac{5^-}{2}$ | $\frac{7^-}{2}$ | 0.075[a] | 0.34±0.10 | 41.4 | 0.35 | 0.17 | 0.015 | 0.0084 | ··· |
| $Fe^{57}$ | 136.4 | $\frac{1^-}{2}$ | $\frac{5^-}{2}$ | 0.043[b,c] | 12.7 ±0.5 | 120 | ··· | ··· | ··· | ··· | 12.0 |
| $Zn^{67}$ | 184 | $\frac{5^-}{2}$ | $\frac{5^-}{2}$ | 0.032[a] | 1.45±0.15 | 11.6 | 1.69 | 0.063 | 0.014 | 0.15 | ··· |
| $Ge^{73}$ | 67.03 | $\frac{9^+}{2}$ | $\left(\frac{11^+}{2}\right)$ | 0.084[a] | 2.33±0.20 | 696 | 2.88 | 2.85 | 0.222 | 0.0041 | ··· |
| $Se^{77}$ | 246 | $\frac{1^-}{2}$ | $\left(\frac{3^-}{2}\right)$ | 0.17[d] | 0.10±0.05 | 1.05 | 0.11 | 0.03 | 0.0096 | 0.11 | ··· |
| $Mo^{95}$ | 203 | $\frac{5^+}{2}$ | $\frac{3^+}{2}$ | 0.035[c,e] | 1.03±0.10 | 4.18 | 1.46 | 0.086 | 0.036 | 0.35 | ··· |

[a] See reference 8.
[b] See reference 9.
[c] These reduced transition probabilities have been corrected for internal conversion.
[d] *Nuclear Data Sheets* (National Academy of Sciences, National Research Council, Washington, D. C., 1959).
[e] See reference 14.

[7] K. Alder, A. Bohr, T. Huus, B. Mottelson, and A. Winther, Revs. Modern Phys. **28,** 432 (1956).

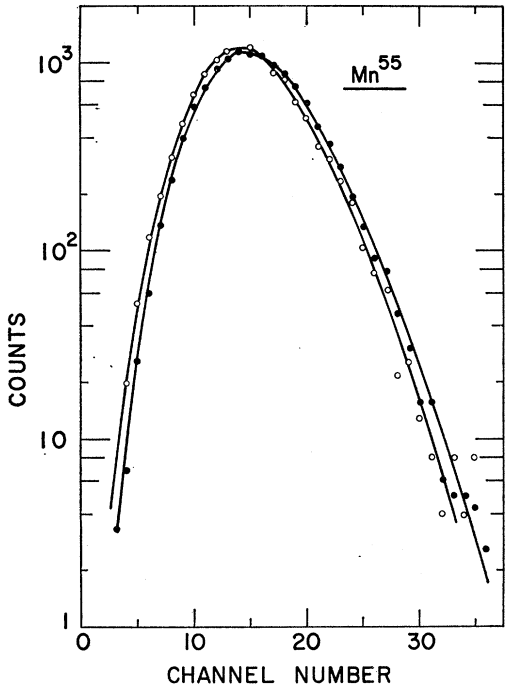


FIG. 1. Time spectra from Mn target showing the prompt curve (open circles), delayed curve (closed circles), and the least-squares fit to the delayed curve. One channel is equivalent to 0.50 mμsec.

When direct evidence on the spin of the excited state was not available, we used the value given in parentheses. For $B(E2)$, we took the published value which seemed most reliable. Conversion coefficients for these transitions are small and were obtained by interpolation in Rose's tables.[2]

### (1) Titanium-47

A 0.010-in. foil of normal titanium bombarded with $\alpha$ particles showed very clearly the 160-kev gamma ray[8] associated with the first excited state of $Ti^{47}$. The Compton spectrum due to higher energy gamma rays from Coulomb excitation of states in the even titanium isotopes was not large, and no corrections were made for it. Since only the 160-kev gamma ray was present, time spectra were also taken with a plastic phosphor. These were in agreement with the NaI data. The average of all measurements was a mean life of $0.32\pm0.10$ mμsec. Using Eq. (1), we have calculated the partial $M1$ mean life, $\tau(M1)=0.326$ mμsec, and the ratio of $E2$ to $M1$ transitions, $E2/M1=0.013$.

### (2) Manganese-55

A chip of manganese metal, when bombarded with $\alpha$ particles, emitted the 128-kev gamma ray[8] associated with the first excited state of $Mn^{55}$. Compton events from higher energy gamma rays due to reactions or impurities were not numerous and were neglected. Again data with a plastic phosphor agreed with the data from NaI. Data obtained with a NaI detector are shown in Fig. 1. The average of several measurements gave a mean life of $0.34\pm0.10$ mμsec.

### (3) Iron-57

A 0.010-in. iron foil, when bombarded with $\alpha$ particles, showed the 122-kev gamma ray associated with the second excited state of $Fe^{57}$ at 136 kev. The data for this gamma ray were taken with rf deflector frequencies of 2.0 Mc/sec and 3.5 Mc/sec. Since the lifetime is so long, the usual alternation of targets was not used but a short run was taken after the iron data with a Ta target to show the position of the prompt peak. Analysis was made by a least-squares fit to the tail of the time spectrum, although all methods described in Sec. III gave results within the assigned error. The time spectra are given in Fig. 2. The average of all measurements of the mean life was $12.7\pm0.5$ mμsec.

We can also calculate the lifetime of this state from the Coulomb excitation cross section and the branching ratio of the 122-kev and 136-kev transitions, if we assume that the 136-kev transition is pure $E2$. The observed transition rate should be given by

$$\lambda(\text{obs})=\lambda_{122}(1+\alpha_{122})+\lambda_{136}(1+\alpha_{136}). \quad (3)$$

Ferguson, Grace, and Newton[9] obtained the branching ratio

$$\lambda_{122}/\lambda_{136}=8.6\pm0.2,$$

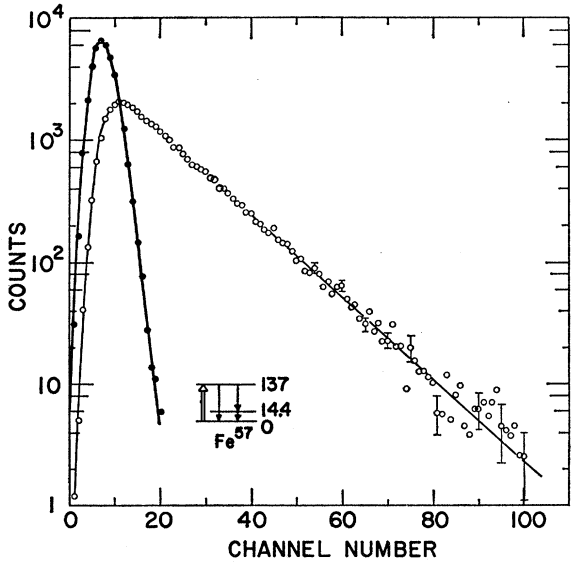


FIG. 2. Time spectra from Fe target showing the prompt curve (closed circles), delayed curve (open circles), and the least-squares fit to the tail of the delayed curve. One channel is equivalent to 1.00 mμsec.

[8] G. M. Temmer and N. P. Heydenburg, Phys. Rev. **104**, 967 (1956).

[9] A. T. G. Ferguson, M. A. Grace, and J. O. Newton, Nuclear Phys. **17**, 9 (1960).

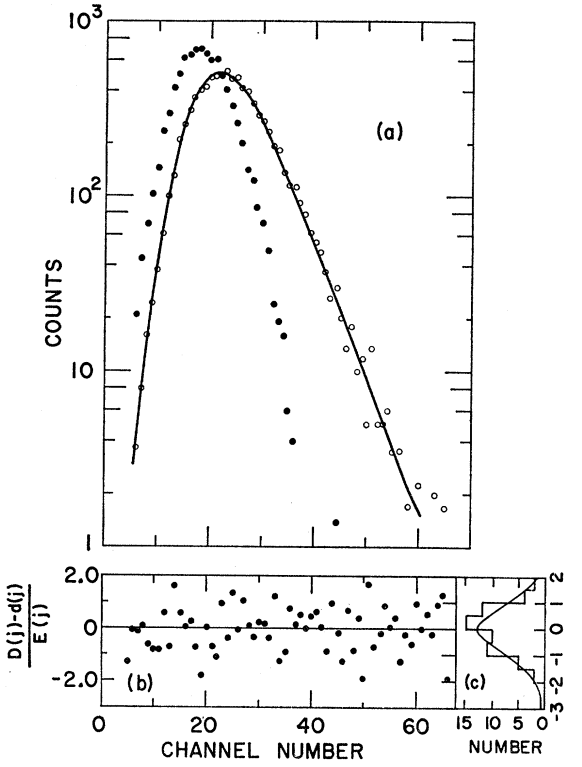


FIG. 3. (a) Time spectrum obtained with a Zn target showing the prompt curve (closed circles), delayed curve (open circles), and least-squares fit to the delayed curve. One channel is equivalent to 0.262 mμsec. (b) The difference between the calculated curve and experimental points of (a) divided by the expected error, plotted as function of time. (c) A frequency curve of the errors of (b) plotted against the error. The Gaussian curve which should be expected is also shown.

and reduced upward transition rate

$$B(E2)=(0.043\pm0.005)\times10^{-48}\ \text{cm}^4.$$

We obtained internal conversion coefficients by interpolation in Rose's tables[2]:

$$\alpha_{122}=0.028 \quad \text{and} \quad \alpha_{136}=0.152.$$

When we insert these values in Eq. (3), we find

$$\lambda(\text{obs})=12.0\pm1.4,$$

in good agreement with our value of $12.7\pm0.5$ and the value $12.5\pm0.5$ obtained by Ferguson *et al.*[9]

### (4) Zinc-67

When a thin plate machined from reagent grade zinc was bombarded with 3.3-Mev $\alpha$ particles, it showed the 184-kev gamma ray as well as an indication of the two gamma rays at 90 kev. Figure 3(a) gives results of a measurement and shows in addition the time spectrum of the prompt gamma ray from a lithium target. The solid curve is the best least-squares fit calculated according to Sec. III. The difference between the experimental points $D(j)$ and the calculated line $d(j)$ divided by the statistical error expected from the number of counts is given in Fig. 3(b). No systematic behavior is seen. Figure 3(c) shows a histogram of the distribution of errors, which should be a Gaussian curve, and, for comparison, the expected Gaussian curve. The value of $\chi^2$ for this set of data is 44 compared to the expected value of 61. In general, the values of $\chi^2$ are higher than the expected value but seldom above the 2% expectation.

The calculation of partial transition rates is complicated for this case by the two modes of decay (either 91-kev or 184-kev radiation). The observed transition rate can be written as

$$\lambda(\text{obs})=\lambda_{184}[1+\alpha_T(184)]+\lambda_{91}[1+\alpha_T(91)], \quad (4)$$

where $\lambda_{91}$ and $\lambda_{184}$ are partial transition rates for emission of a gamma ray of the corresponding energy. We know from the relative numbers of gamma rays emitted by this state that

$$\lambda_{184}/\lambda_{91}=11.5, \quad (5)$$

where we have averaged measurements by Meyerhof *et al.*,[10] Ketelle *et al.*,[11] and Rietjens *et al.*[12] By using the measured value $\alpha_T(91)=0.074$ and Eq. (5) in an iterative procedure, we can find the partial rates $\lambda(M1)$ and $\lambda(E2)$ for the 184-kev gamma ray. The corresponding partial mean lives for the 184-kev transition are given in Table I.

### (5) Germanium-73

A chip of metallic germanium was bombarded with $\alpha$ particles. It showed the strong gamma ray at 68 kev first observed by Temmer and Heydenburg.[8] By using the lead x ray as the prompt gamma ray, we obtained a mean life of $2.33\pm0.20$ mμsec.

### (6) Selenium-77

Gamma rays of 246 and 457 kev were observed as well as some unresolved lines of lower energy from a target of pressed Se powder. The photopeak at 246 kev showed a small shift of centroid corresponding to a mean life of $0.10\pm0.05$ mμsec.

### (7) Molybdenum-95

A 0.010-in. foil of molybdenum showed the 204-kev gamma ray from $Mo^{95}$ as well as some Compton events from higher energy gamma rays. We obtained a mean life of $1.03\pm0.1$ mμsec. A previous measurement on $Mo^{95}$ has been given by Quidort[13] as 1.10 mμsec.

[10] W. E. Meyerhof, L. G. Mann, and I. H. West, Jr., Phys. Rev. **92**, 758 (1953).
[11] B. H. Ketelle, A. R. Brosi, and F. M. Porter, Phys. Rev. **90**, 567 (1953).
[12] L. H. Th. Rietjens and H. J. Van den Bold, Physica **21**, 701 (1955).
[13] J. Quidort, Compt. rend. **246**, 2119 (1958).

McGowan and Stelson[14] also obtained a mean lifetime of 1.10 mμsec from angular distribution measurements.

### (8) Tantalum-181

Measurements were also made with a tantalum target to check on the reliability of our procedures. The level at 137 kev is known to have a mean life of 0.06 mμsec from the work of Blaugrund, Dar, and Goldring.[15] The mean life of 0.04 mμsec obtained by us as an average of 50 measurements taken at various times indicates the average of the systematic errors is very small. The sources of these errors are discussed in Sec. V.

## V. SOURCES OF ERROR

The statistical accuracy of these measurements is usually good enough so that the main sources of error were due to a number of systematic effects. The origins and magnitudes of these errors as well as methods of reducing them are discussed below and summarized in Table II. In this table, column one gives the source of error; column two, the largest correction applied to any of the centroid shift calculations from this source; column three, the estimated error in the measurement corrected according to column two. Several of the errors (c, g, and h) become less serious as the energy of the gamma ray approaches that of the prompt gamma ray. The errors assigned to the measurements are standard deviations and are based both on internal consistency and on our estimate of the systematic errors. Since the latter vary considerably depending on the energy of the gamma ray and the complexity of the gamma-ray spectrum, the assigned errors show considerable variation.

TABLE II. Sources of error. A more complete discussion of each source of error is given in the text. The first column gives the source of error; the second, the correction applied to centroid calculation; the third, the estimated error in the corrected data from this source.

| Source of error | Typical correction | Typical estimated error |
|---|---|---|
| (a) Electronic | ··· | 0.03 mμsec |
| (b) Window position | 0.1 mμsec | 0.03 mμsec |
| (c) Scattering | 0.04 mμsec | 0.03 mμsec |
| (d) Complex spectra | 10% | 2% |
| (e) Calibration, etc. | ··· | 2% |
| (f) Target position | ··· | <0.01 mμsec |
| (g) Nonuniform scintillation | ··· | 0.05 mμsec |
| (h) Čerenkov radiation | ··· | <0.02 mμsec |

### (a) Electronic Equipment

Effects in the electronic equipment may alter both the shape and the displacement of the time spectra (centroid shift). Since the electronic equipment is ac coupled, bias changes occur in amplifiers and trigger circuits at high counting rates and these changes lead to a spurious centroid shift. Mean lives reported in this paper were measured with several values of beam current, the usual current leading to a spurious shift of less than 0.03 mμsec.

### (b) Effective Window Position

The distribution of pulses in the slow-channel "window" may not be the same for the two targets. Such a difference in the effective window positions for the two targets can lead to a 0.2 mμsec error in the centroid calculation for a slow-channel window width of 15%. We have corrected for this error in one of two ways. In the first method, a lifetime measurement was made with a series of windows of different size to make sure that at the smallest window the effect was negligible. In the second method, we recorded the distribution of pulses in the slow-channel window. The center of gravity of these distributions gives the effective window level. Then by using an experimentally determined curve of centroid position vs window level, we computed a correction to the centroid difference. The methods gave results in good agreement. The data shown in the figures were taken with a window small enough so that this effect was less than 0.03 mμsec.

### (c) Scattering

When the prompt and unknown gamma rays differ sufficiently in energy, then the higher energy one can be scattered and still have sufficient energy to fall in the single-channel window. The largest part of such events in our arrangement come from the shield box installed to reduce the x-ray background from the accelerator. These events are delayed a few millimicroseconds and are numerous enough to shift the centroid 0.2 mμsec when the distance from target to detector is $1\frac{1}{2}$ in. and one is comparing a 160-kev gamma ray to the 480-kev prompt gamma ray. For window levels below 100 kev, multiple scattering in the box becomes important and the effect becomes much more pronounced. This error was minimized by taking data with the detector at the closest practicable distance ($\frac{1}{4}$ in.) from the target and then estimating the effect by repeating the measurement at 1 in. The resulting correction was less than 0.04 mμsec. This procedure is not effective in estimating the effect of gamma rays scattered from the target holder. However, data taken with various target holders of various masses showed no effect larger than the statistical accuracy of 0.03 mμsec.

### (d) Complex Gamma-Ray Spectra

When more than one gamma ray is emitted by the target, it is not possible with a NaI detector to select

[14] F. K. McGowan and P. H. Stelson, Phys. Rev. **109**, 901 (1958).
[15] A. E. Blaugrund, Y. Dar, and G. Goldring, Phys. Rev. **120**, 1328 (1960).

events due to only one of the gamma rays, except for the one of highest energy. However, the number of unwanted events could be estimated from the pulse-height spectrum. If they were prompt, they were subtracted before the least-squares fitting was performed. In some cases, uncertainty as to the lifetime and number has forced us to increase the error assigned to our measurement.

### (e) Calibration of the Time Scale

The time-to-pulse-height converter was calibrated daily in terms of the rf period of the deflector, as described in Sec. II. Variation in converter calibration leads us to assign an upper limit of 1% to errors from this source. The error due to nonlinearity of the converter is taken as 2%.

### (f) Effective Position and Uniformity of Targets

The target position (the point at which the beam impinges on the target) was constant to 0.005 in. so that the errors from this source were less than 0.01 m$\mu$sec. A nonuniform target could also easily lead to large errors. Although we had no reason to suspect such a nonuniformity in either the solid targets or the evaporated targets, this effect was checked both by inverting one target and by using the other peak in the time spectrum, where the order of sweeping is inverted. In all cases, no difference larger than the statistical error was observed.

### (g) Effects in Scintillator and Phototube

Gamma rays of different energy are absorbed at different rates in the scintillator. Thus a variation in scintillator efficiency, or in the manner in which the photocathode was illuminated, could lead to a systematic error. Such an effect is difficult to calculate or to measure. We have observed a small effect which depends on scintillator size and a larger effect which depended on the orientation of a particular scintillator with respect to the phototube. There was a repeatable and consistent difference in position of the centroid of 0.05 m$\mu$sec depending on orientation of the scintillator relative to the photocathode when comparing the tantalum 137-kev gamma ray with the 480-kev gamma ray from Li.

### (h) Čerenkov Radiation

An effect due to Čerenkov radiation in the scintillator should be expected when comparing gamma rays of different energy. This arises in the following manner. We compare the time spectra of a portion of the Compton pulses from the higher energy (prompt) gamma ray with pulses in the photopeak of the lower energy gamma ray. All pulses which are above the threshold for the Čerenkov effect (108 kev in NaI) will have some Čerenkov radiation (which is very fast) associated with them. However, some of the pulses in the Compton spectrum will have more than the normal amount of Čerenkov radiation because they are due to higher energy electrons which escaped from the scintillator. For these events, the fast circuit will "see" a higher number of electrons from the photocathode and will therefore trigger earlier than it would on a "normal" pulse. This in turn leads to an anomalous number of early pulses in the prompt time spectrum. This effect would be particularly annoying in centroid computations.

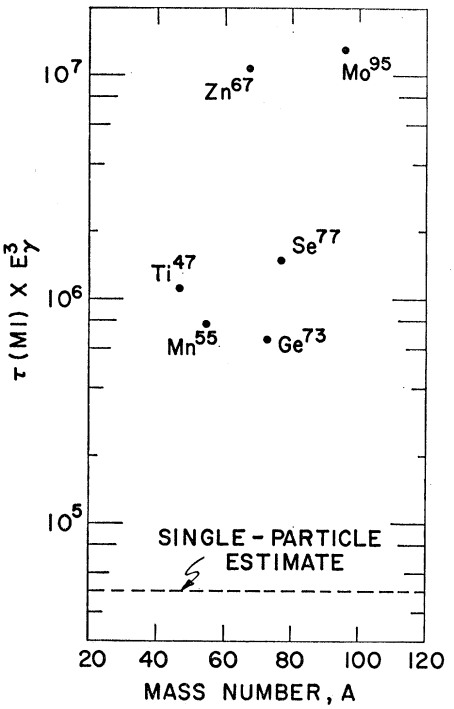


FIG. 4. Reduced partial $M1$ mean life plotted as a function of atomic number.

We have observed such an effect, highly exaggerated, when comparing a 1600-kev prompt gamma ray with a 450-kev one. As one would expect, the fraction of early pulses was strongly dependent on the size of the scintillator. A computation, which involved several simplifying assumptions, gave results in fair agreement (within 50%) with the data obtained with these high-energy gamma rays. On the basis of these computations the effect for the measurements reported here was estimated to be less than 0.02 m$\mu$sec.

The magnitude of this effect decreases the closer the energy of the two gamma rays, the larger the scintillator, and the faster the scintillator. An effect which is probably due to Čerenkov photoelectrons was observed by Bell and Jorgensen[16] while using diphenylacetylene scintillators.

[16] R. E. Bell and M. H. Jorgensen, Nuclear Phys. **12**, 413 (1959).

## VI. DISCUSSION

Figure 4 shows the reduced partial $M1$ mean life plotted with respect to mass number. The single-particle estimate of Moszkowski is shown as a horizontal line. In this very small sample there appear to be two groups, one about 20 times the single-particle estimate. Preliminary results on slightly heavier nuclei show some cases that fall between the two groups. The group of longer lifetime have the same reduced lifetimes as the group of $L$-forbidden transitions measured by DeWaard and Gerholm.[17]

In general the reduced partial $M1$ mean lives fall in the same region as among the heavy elements, and are somewhat longer than those found in the light elements.[18]

## ACKNOWLEDGMENTS

We are indebted to A. Vandergust for construction and maintenance of much of the equipment, and to J. Wallace and the Van de Graaff group for operation of the electrostatic accelerator. Dr. J. Monahan made several statistical analyses of our data and helped us program them for the IBM-704 computer. Dr. E. N. Shipley helped in taking some of the data and coded the computer program to fit the tail of the time spectra by least squares.

[17] H. DeWaard and T. R. Gerholm, Nuclear Phys. **1**, 281 (1956).

[18] D. H. Wilkinson, Phil. Mag. **1**, 1031 (1956); *Proceedings of the Rehovoth Conference on Nuclear Structure*, edited by H. J. Lipkin (North-Holland Publishing Company, Amsterdam, 1958), p. 175; *Nuclear Spectroscopy*, edited by Fay Ajzenberg-Selove (Academic Press, Inc., New York, 1960), Part B, p. 852.

PHYSICAL REVIEW VOLUME 121, NUMBER 5 MARCH 1, 1961

# Radiochemical Study of the Ranges in Metallic Uranium of the Fragments from Thermal Neutron Fission*

JAMES B. NIDAY
*Lawrence Radiation Laboratory, University of California, Livermore, California*
(Received September 23, 1960)

The mean ranges in uranium of 28 fission products have been determined by radiochemical measurement of the fraction escaping from the surface. Several factors affecting the precision and accuracy of the method are discussed. A semiempirical equation was developed which gave an excellent correlation between the ranges of fragments from a specific mass chain and their average initial velocity. The average total kinetic energy of the fragment pairs is about 30 Mev less for the products of symmetrical fission than is expected from comparison with the asymmetrical products. The low momenta of the symmetrical fragments are not readily explained by particle emission unless the concept of isotropic neutron evaporation is abandoned. The results may be interpreted by assuming that the symmetrical and asymmetrical products result from two modes of fission which involve different critical shapes of the fissioning nucleus, and that the choice between modes is dependent on the closing of the 50-proton shell in the heavy fragment. The 10% decrease in range observed for two shielded nuclides is also examined in some detail.

## I. INTRODUCTION

MANY studies have been made of the ionization produced by fragments from various types of fission and a few studies of the ranges of various fragments in light mass absorbers. Previous work on the kinetic energies of fission fragment recoils was summarized by Walton in 1957.[1]

Most of the previous radiochemical work has involved considerable experimental difficulty in the handling of many samples collected in very thin absorbers. In 1955, a preliminary survey of the ranges of some of the fragments formed in the fission of uranium by high-energy particles was begun by a different technique which gives the mean range of a specific mass chain in metallic uranium. This method is based on radiochemical determination of the fraction of the fission fragments escaping from the surface of a "thick" fission source of known area.[2] These exploratory measurements did not readily lend themselves to interpretation, and it was decided to initiate a calibration program during which the reproducibility of this method could be studied. Since range measurements on fission produced by high-energy particles are affected by center-of-mass motion and by anisotropic angular distribution of the fragments, it was felt that the method should give results reliable to about $\pm 1\%$ to permit adequate interpretation.

Measurement of the ranges of fragments from thermal neutron fission of $U^{235}$ offered a convenient means of evaluating other experimental variables, and these

* This work was performed under auspices of the U. S. Atomic Energy Commission.

[1] G. N. Walton, *Progress in Nuclear Physics* (Butterworths—Springer, London, 1957), Vol. 6, pp. 192–232.

[2] This "integral range method" has been used by Batzel, Sugarman, and others in studies of high-energy recoil fragments. See, e.g., R. E. Batzel and G. T. Seaborg, Phys. Rev. **82**, 607 (1951); and N. T. Porile and N. Sugarman, Phys. Rev. **107**, 1410 (1957).